Composites Part C: Open Access 8 (2022) 100287

Contents lists available at ScienceDirect

Composites Part C: Open Access

journal homepage: www.sciencedirect.com/journal/composites-part-c-open-access

Experimental investigation into the direct feeding of coupling agent, cellulose nanocrystals, and nano zinc oxide in high-density polyethylene

Ghazal Vahidi [a], Dilpreet S. Bajwa [a,*], Jamileh Shojaeiarani [b], Nicole M. Stark [c]

[a] Department of Mechanical and Industrial Engineering, Montana State University, Bozeman, MT 59717, USA
[b] Mechanical Engineering Department, Western New England University, Springfield, MA 01119, USA
[c] Forest Products Laboratory, USDA Forest Service, Madison, WI 53726, USA

ARTICLE INFO

Keywords:
Nanocomposites
High density polyethylene
Cellulose nanocrystals
Zinc oxide
Maleic anhydride

ABSTRACT

High density polyethylene (HDPE) is widely used in composite industry as a host polymer because of its low cost and competitive mechanical properties. However, the addition of hydrophilic reinforcing nanofillers in HDPE-based composites is challenging and often requires chemical treatment. This study explored the addition of coupling agent maleic anhydride (MA) for improving the dispersion of cellulose nanocrystals (CNCs) and nano zinc oxide (ZnO) in HDPE matrix, using two separate methods. MA grafted HDPE (MAPE) and HDPE with MA powder (HDPE-MA) were melt compounded with CNCs and ZnO. These nanofillers has been of recent interest due to their superior properties, wide availability, and biocompatibility. Physical and mechanical properties of the composite samples were studied using different characterization techniques (FTIR, SEM, DMA, Tensile and Rheology). Overall, composites with HDPE-MA showed improved adhesion between fillers and matrix, compared to the MAPE composites. Furthermore, using CNCs and ZnO in powder form and separately, displayed better interactions between nanoparticles and HDPE matrix, indicating improved energy dissipating properties. HDPE-MA composites showed relatively similar values for mechanical properties compared to the virgin HDPE, however, adding nanofillers into MAPE increased the maximum tensile strength up to 42% but lowered the Young's modulus. The addition of nanofillers increased the complex viscosity for HDPE-MA nanocomposite whereas decreased this measure for MAPE nanocomposites, compared to their respective virgin polymers. Similarly, loss and storage moduli improved for HDPE-MA nanocomposites and declined for MAPE nanocomposites compared to their respective virgin polymers.

1. Introduction

Engineered polymer composites with enhanced characteristics, have attracted a lot of interest as an effective replacement for traditional metallic components. Traditionally, polymer matrices have been reinforced by adding micro sized fibers or fillers, however nano sized fillers (1–100 nm at least in one dimension) are now making inroads [1]. Composites with nano sized fillers are being used in various industrial sectors, especially in automotive, biomedical, building materials, and aerospace [2]. Thermoplastic polymers such as polyolefins and polyamides are among the most representative choices as a matrix material in nanocomposites owing to ease of processing, recyclability, superior mechanical properties, and cost-effective manufacturing methods [3].

High-density polyethylene (HDPE) is one of the most widely used thermoplastic polymers due to its low cost, high strength-to-density ratio, and recyclability. The introduction of nanoparticles into HDPE may improve the mechanical and thermal properties of the resulting nanocomposites. Hydrophobic properties of HDPE have prevented the uniform dispersion of hydrophilic nanoparticles. In nanocomposite manufacturing, since direct mixing of nanofillers and polymer is preferred, much research is focused on finding suitable compatibilizers to enhance the interfacial attraction between polymer and nanoparticles. [4].

The excellent mechanical properties of cellulose nanocrystals (CNCs) due to their high aspect ratio and highly crystalline structure, make them ideal candidates as reinforcing fillers for polymeric matrices [5,6]. There are major difficulties to disperse CNCs effectively into a thermoplastic polymer such as HDPE during melt processing due to their non-compatibility with polymer. Different feeding of nanoparticles have been suggested to overcome the compatibility issues of nanofillers.

* Corresponding author.
E-mail address: Dilpreet.bajwa@montana.edu (D.S. Bajwa).

https://doi.org/10.1016/j.jcomc.2022.100287

Available online 2 June 2022

Silane treatment has been used both in polyolefin-cellulose composites [7,8] and HDPE-wood composites to enhance compatibility [9]. Other methods have been focused to improve dispersing CNCs in nonaqueous solvent such as using surfactants [10] or template approaches [11]. Although these methods usually report an improved dispersion of nanofillers, they are expensive and non-functional for industrial-scale productions.

The addition of compatibilizer or coupling agent such as maleic anhydride (MA) is one other option to enhance the interactions between HDPE and CNC via an esterification reaction and hydrogen bonding of MA functional groups (-COOH and -C=O) and cellulose hydroxyl groups (-OH) [12]. MA grafted polymers including polyethylene and poly lactic acid have shown improved compatibility with natural fibers [13,14]. In a study, a composite of HDPE with microcrystalline cellulose and viscose fibers was prepared via melt-mixing using maleic anhydride grafted polyethylene as a polymeric compatibilizer [15]. The resulting composite had improved dispersion of the fillers and increased thermal stability. In another study, cellulose composites that were prepared with maleated low density polyethylene showed improved yield stress and elongation compared to cellulose composites prepared with only low density polyethylene, showing the compatibilizer effect of maleic anhydride [16].

Zinc oxide has been used in polymer composites to improve the mechanical properties, photocatalytic activity, and antibacterial properties of the materials [17,18]. Recently nano zinc oxide has been added to polypropylene to improve durability and antibacterial properties [19]. Nano-sized ZnO can be synthesized through simple, fast, and cost effective laboratory methods [20]. Due to the high exciton bonding energy along with the large width of band, these nanoparticles have lots of potential applications such as anti-inflammatory, wound healing and antioxidant properties [21]. In comparison to micro-sized ZnOs, nano-sized ZnO has smaller dimensions and a larger specific area, which can result in stronger interfacial interactions when compounded with other [22]. Strong interfacial interaction between nano ZnO, CNCs and polymer matrix and uniform dispersion of nanofillers is highly desirable as it can result in superior performance of composites compared to the virgin polymer.

This study aimed to investigate a chemical-free, effective, and efficient method for dispersing CNCs and nano zinc oxide in the HDPE matrix. Both of these fillers have been of recent interest due to their superior properties, wide availability and biocompatibility, however, their application in hydrophobic polymers such as HDPE has been limited due to lack of compatibility and expensive dispersion methods. Here, CNCs and coupling agents coated with ZnO were introduced into the HDPE matrix using a high-shear melt compounding technique. The influence of feeding MA via different mechanisms on the dispersion of nanoparticles and their impact on the physical and mechanical properties of nanocomposites was evaluated.

2. Materials and methods

2.1. Materials

High density polyethylene (HDPE Marlex-9006, MFI: 6 g/10 min, density: 0.953 g/cm^3) was purchased from Chevron Philips chemicals (woodland, TX). Cellulose nanocrystals (CNCs, dimensions of 150 nm length and 7 nm width) extracted from pinewood-based cellulose via acid hydrolysis were supplied by US Forest Product Laboratory (Madison, WI). Maleic anhydride (MA, $C_4H_2O_3$, purity $\geq$ 99.0% (NT), M_w = 98.06 g/mol) was purchased from Sigma-Aldrich chemicals (St. Louis, MI), and dibenzoyl peroxide as the initiator ($C_{14}H_{10}O_4$, 75% remainder water, M_w = 242.23 g/mol) was obtained from Acros Organics (Morris, NJ).

2.2. Nanocomposite processing

Zinc oxide nanoparticles were prepared following the procedure described in previous reports [23]. Briefly, 13.17 g sodium hydroxide powder was dissolved in 300 ml methanol using magnet stirring for 1 h at 50 °C. Then 9.6 g zinc acetate dehydrate, as the source of ZnO, was dissolved in 300 ml methanol by continuous stirring. The zinc acetate dehydrates mixture was heated to 50 °C, while vigorously stirring for 30 min. The zinc oxide nano-sol started to form by gradually adding zinc acetate solution to sodium hydroxide solution under continuous stirring for 30 min. The mixture was then heated to 50 °C for 30 min and then stirred continuously for 2 h at room temperature to create the ZnO white sol-gel (450 g sol-gel, 9 wt.%). The suspension was dried under a fume hood for 24 h and the ZnO coated CNC films were then grounded in a mortar and pestle to obtain a fine powder which was stored at room temperature.

Two different approaches were used to feed the nano fillers into the polymer matrix, first CNCs and nano ZnO as individual components and second as ZnO—CNC films. (**Fig. 1**). Formulations with individual fillers as powdered CNCs and nano ZnO were marked with "P" (powder), and formulations with filler derived from the ZnO coated CNCs film were marked with "F" (film).

The coupling agent was added to nanocomposites using two different approaches. In the first approach, HDPE pellets were directly fed to a twin-screw extruder along with maleic anhydride (MA, 3 wt%), CNCs, and ZnO either in form of film (F) or powder (P), 3–5 wt% each. In the second approach, maleic anhydride grafted polyethylene (MAPE) was first synthesized via *in situ* polymerization. HDPE pellets with 3 wt% of MA and 0.5wt% of dibenzoyl peroxide were fed to the extruder to synthesize MAPE. MAPE was extruded with CNC and ZnO fillers (3–5 wt% each). Two forms of nanofiller were incorporated into the experiment at two levels (3, 5%) as well as two modes of feeding the coupling agent.

All the materials were mixed thoroughly with an overhead stirrer prior to extrusion using a twin-screw extruder (Krauss-Maffei Co., Florence, KY, USA). The extruder's screw speed was set at 160 rpm and temperatures were ranged from 160 °C to 175 °C (feeding throat to die). Extrudates were collected in filament form with 2 mm diameter and then chopped into small pieces with 2 mm length. A mini-injection molding machine (Mini-Jector 45-OH, USA) at 50 atm pressure and 160°C platen temperature was used to mold nanocomposite pellets into standard dog-bone (ASTM D638–14 standard) [24] and flexural shapes (ASTM D5026) [25]. The final compositions are shown in **Table 1**.

2.3. Nanocomposite characterization techniques

2.3.1. Fourier transform infrared (FTIR) spectroscopy

FTIR measurements of nanocomposite samples were carried out to monitor the formation of new bonds through modification of CNCs as well as the effect of MA as a coupling agent on nanocomposite samples with an absorbance mode in the range of 650–4000 cm^{-1}. A Thermo Nicolet 8700 spectrometer (Thermo Fisher, Waltman, MA, USA) equipped with an attenuated total reflectance (ATR) sampling accessory was used to record the spectra.

2.3.2. Scanning electron microscopy (SEM) of composites

The morphology of HDPE and nanocomposites was studied using scanning electron microscopy (SEM). Representative flexural samples from each formulation were fractured, using an Izod impact tester (Tinius Olsen, Model Impact 104, PA, USA) to produce fracture surfaces for SEM analysis. The impact-fractured surface was investigated using SEM (JEOL Inc., Peabody, MA, USA) working with an accelerating voltage of 20 kV at magnifications of 90X, 300X, and 1000X. The samples were sputter-coated with a layer of gold before SEM examination to avoid specimen excessive charging.

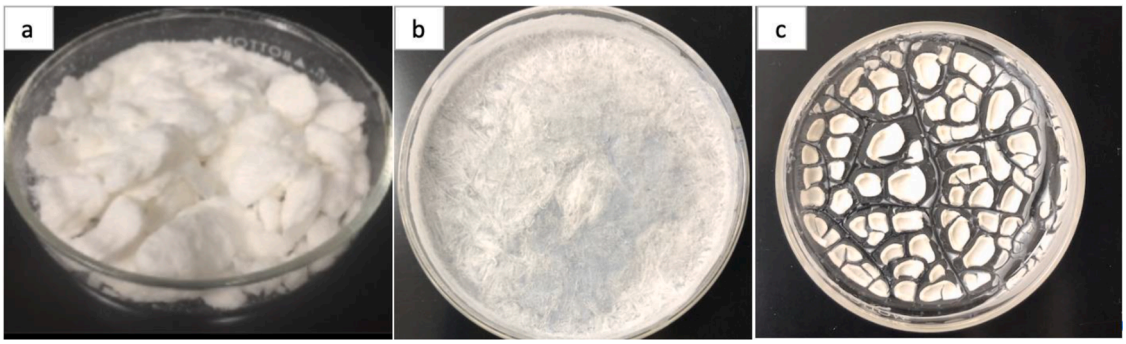

Fig. 1. CNCs and ZnO nanofillers in powder and film forms: a) CNCs powder b) Nano ZnO solution c) CNCs-ZnO film before grinding.

Table 1
Formulations for direct feeding of HDPE and MA or MAPE (with initiator) with ZnO coated CNCs. Same formulations were used for both forms (i.e., powder or film) of CNCs-ZnO.

Material formulation	HDPE (wt %)	CNCs (wt %)	ZnO (wt %)	MA (wt %)	Initiator (wt %)
HDPE-MA-3CNCs-3ZnO	91	3	3	3	–
HDPE-MA-5CNCs-5ZnO	87	5	5	3	–
MAPE-3CNCs-3ZnO	90.5	3	3	3	0.5
MAPE-5CNCs-5ZnO	86.5	5	5	3	0.5

2.3.3. Rheological properties

The flow properties (rheological properties) such as complex viscosity and shear moduli of the formulations were measured using a Rheometer AR 2000 (TA Instruments, New Castle, DE, USA). The rheological properties of HDPE and nanocomposites were measured in an oscillatory mode in frequency sweep test setup. 0.5 g of the sample was placed between two parallel plates with a 25 mm diameter and a 1 mm gap at 180 °C.

2.3.4. Dynamic mechanical analysis (DMA)

A dynamic mechanical analyzer (TA Instruments, DMA Q800, DE, USA) was used to investigate the viscoelastic behavior of nanocomposites. DMA was equipped with a dual cantilever clamp according to ASTM D5026 [25] to study viscoelastic behavior of the nanocomposite. Temperature was set in the range of 40–120 °C at a heating rate of 1 °C min^{-1}. DMA samples were prepared with approximately 59 mm length, 13 mm width, and 3 mm thickness. The test was repeated twice for each formulation.

2.3.5. Mechanical properties (Tensile test)

Mechanical characteristics of injection molded samples, including ultimate tensile strength, strain at maximum tensile strength, and modulus of elasticity, were evaluated from tensile test following ASTM D638–14 standard [24]. An Instron universal testing machine (Model 5567, Norwood, MA, USA) was used at room temperature (25 °C) to investigate the mechanical properties of the composite samples compared to the virgin polymer. Instron machine was equipped with a 2 KN load cell and the crosshead speed was set at 5 mm/min. Four samples for each group of composites and pure polymers ($n = 40$ in total) were tested. Data were reported as mean and standard deviation for each group. The main effects of polymer type (HDPE-MA polymer groups vs. MAPE polymer groups) and the formulation of composite (Pure polymer vs. 3% film vs. 5% film vs. 3% powered vs. 5% powder), and the interaction between these two terms were assessed on mechanical testing results, using ANOVA (Minitab, State College, PA USA). The model satisfied residual normality and homoscedasticity assumptions. Significance for main effects and interactions was set a priori to $p < 0.05$.

3. Results and discussions

3.1. Fourier transform infrared (FTIR) spectroscopy

FTIR absorption spectra were recorded for determination of the new peaks as a sign of chemical bonding between MA coupling agent, HDPE, and CNCs-ZnO fillers as shown in Fig. 2 The C=O peak, specific to PE and MA chemical bonding, was observed at 1742 cm^{-1} wavenumber for all formulations containing MA. This observation suggested the successful interaction of HDPE with coupling agent [26]; new bands at 1718 cm^{-1} to 1790 cm^{-1} wavenumbers belonged to symmetric and asymmetric stretching of the carbonyl group (C=O) of MA [27]. In MAPE formulations spectra, a new peak was observed at 1100 cm^{-1}, which was assigned to C—O bond in ether alcohol functional groups or benzoic acid compound; this can be a sign of dibenzoyl peroxide decomposition producing either ether or benzoic acid groups [28,29].

In MAPE formulations, a peak at 3350 cm^{-1} indicated that an O—H band existed between the HDPE backbone and peroxide molecule, which initiated the MA grafting process [30].

The FTIR spectra of all formulations with CNCs exhibited a broad band over 3100 to 3500 cm^{-1}, which can be attributed to the O—H stretching vibrations [31]. The intensity of the peak was weaker in HDPE-MA compared to the MAPE formulation, indicating that MA incorporation into CNCs was stronger in these composites compared to MAPE composites. By contrast, MAPE formulations had a peak intensity similar to that of neat CNCs [32]. This might indicate that peroxide inhibited MA from bonding with CNCs in MAPE formulations. The band at 2920 cm^{-1} wavenumber can be contributed to the C—H stretching vibrations existing in HDPE [33]. Additionally, The peaks with 1250 cm^{-1} wavenumber exhibited the bending vibrations of CH_2 saccharide structure in CNCs [20]. The new peak created by successful grafting of ZnO on CNCs at 810 cm^{-1} is related to the out of plane deformations of carboxyl groups in CNCs [34], and this new peak was shifted and weakened compared to the FTIR spectra of neat CNCs from literature [21,33,35]. The subpeak around 850 cm^{-1}, which is a characteristic of C—H stretching and C—O bounding, intensifies with addition of nanofillers which may imply successful grafting of nanofiller on polymer backbone [36–38].

3.2. Scanning electron microscopy (SEM) of composites

The impact-fractured surfaces of the nanocomposites were studied using SEM images as illustrated in Figs. 3 and 4. The HDPE-MA composites with 3 and 5 wt.% powder nanofillers did not show any agglomeration, which can be interpreted as indicating improved adhesive properties between the powdered fibers and the polymer that contains them [35,39]. However, the presence of CNCs-ZnO aggregates was predominant in the film formulations for HDPE-MA composites.

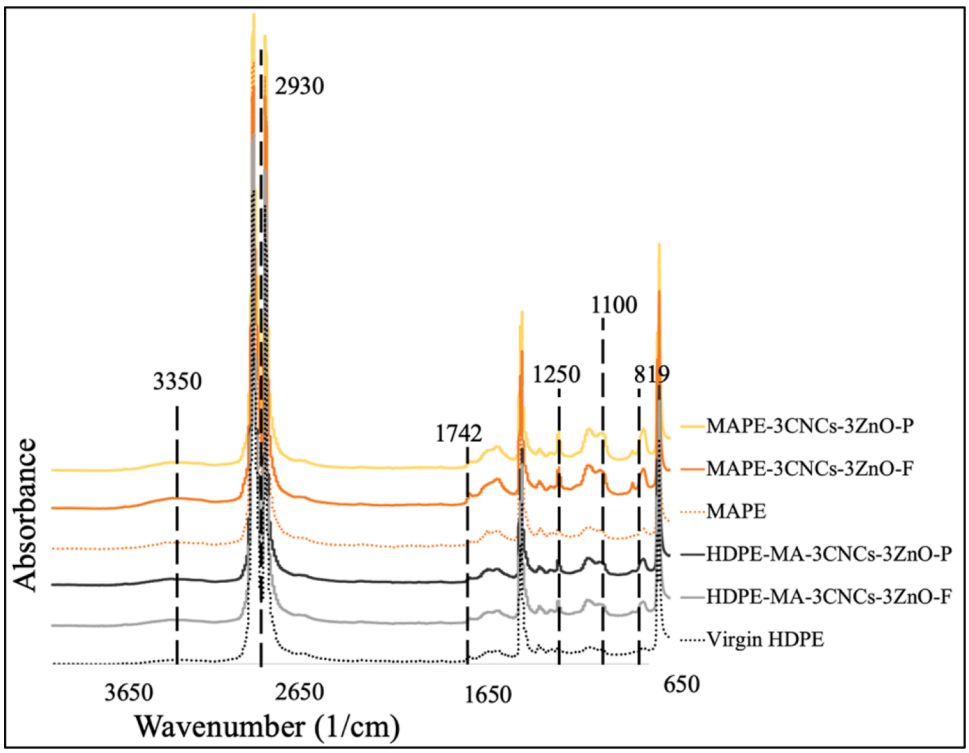

Fig. 2. FTIR spectra of HDPE, MAPE, and their nanocomposites with 3 wt.% filler in absorbance mode.

These aggregates can be seen as white agglomerations with cavities around them, as seen in rows 2 and 4 in Fig. 3. Compared to HDPE-MA formulations, the occurrence of CNCs-ZnO aggregates in MAPE nanocomposites were more prevalent in both powder and film forms, as depicted in Fig. 4. In powder form, particles have an increased surface area for interacting and forming new bonds. This may help increase adhesion between nanofillers and polymer matrix, as has been observed for HDPE-MA nanocomposites.

In HDPE-MA nanocomposites, formulations with 3 and 5 wt.% nanofillers in powder form exhibited a rough surface with irregular patterns, indicating that a higher energy is required for the for fracture to propagate. On the other hand, in formulations with 3 and 5 wt.% nanofillers in film form, the fractured surface was laminated and smoother, suggesting a more brittle nature [22]. The fractured surface in all MAPE formulations was rougher and had more irregular patterns compared to other HDPE-MA formulations, suggesting a more ductile and less stiff nature. It is important to highlight that the results presented here are only qualitative, and the hardness and work necessary for fracture of the composite materials have not been evaluated in-depth.

3.3. *Rheological properties*

Dynamic oscillatory shear measurements were carried out at 180 °C to study the rheological properties and dynamic shearing response of the HDPE-MA, MAPE and the corresponding formulations. Representative complex viscosity (η*) curves for different formulations are shown in Fig. 5. When nanofillers were added to HDPE, the complex viscosity increased; indicating that the nanocomposites had a higher melt strength than virgin polymers. This behavior can be attributed to both the interactions between the matrix and nanofillers and also the formation of the network-like structures, which is most likely due to the MA cross-linking effect [40]; a network structure shows greater resistance to the applied stress. The overall complex viscosity values were observed to be greater at higher concentrations of nanofillers. Due to the presence of nanofillers and their increased interaction with the matrix, the polymer chains were restricted in their mobility in the molten state. This, in turn, caused the nanocomposite to have a higher viscosity than virgin polymer. [41].

It is worth mentioning that the polymer chain structure significantly governs the rheological properties and melt strength of the polymers. By increasing the operating frequency, η* values started to decline for all formulations submitting a non-Newtonian behavior that is called shear thinning effect in molten state [42]. Highly cross-linked structure of MAPE exhibited a higher viscosity compared to the formulations with the nanofillers, in which the addition of the nanofillers caused a chain scission reaction in the matrix and decreased the viscosity [43]. Chain scission produces shorter polymer chains, so they can flow more easily as a result of their increased mobility [44]. It is concluded that the presence of the peroxide in these formulations caused oxidation and degradation of CNCs and subsequently, the chain scission of HDPE.

Rheological behaviors of HDPE and its different formulations were also studied through shear moduli as a function of angular frequency at 180 °C. Fig. 6a displays the storage and loss modulus values for HDPE-MA compared to its nanocomposites. With the addition of nanofillers to virgin HDPE, both storage and loss moduli were improved, suggesting relatively strong interactions between matrix and nanofillers that resulted in more efficient stress transfer. At higher nanofiller loadings, higher storage and loss moduli were observed, most likely due to the enhancements in chain entanglements of the polymers [4]. This finding was in agreement with SEM observations of fractured surface, where addition of nanofillers enhanced the presence of energy dissipating patterns. On the contrary, the addition of nanofillers in MAPE polymer resulted in reduction of both storage and loss moduli (Fig. 6b). This observation may be attributed to the fewer interactions between the nanofibers and the matrix in these formulations and lower viscosity. Moreover, in a study conducted by Shojaeiarani et al., ZnO particles have been reported to have a negative effect on polymer chains and reduce the molecular weight of the nanocomposites [23]. This together with the lower dispersion of nanofillers in MAPE could be the reason for reduced values of storage moduli of MAPE based composites. An increasing trend was observed for storage and loss moduli by increasing the angular frequency for all formulations; During lower frequency

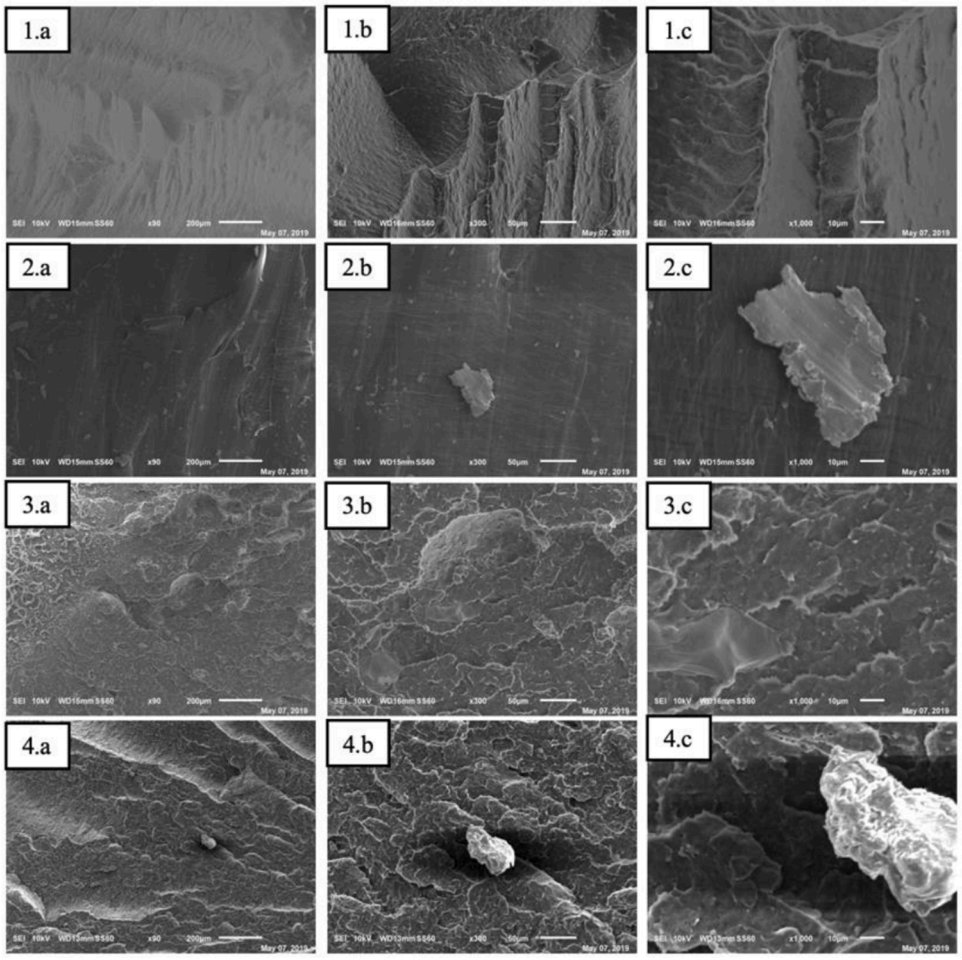

Fig. 3. SEM micrographs at three magnifications a) 90X, b) 300X, c) 1000X for HDPE-MA nanocomposites 1) HDPE-MA-3CNCs-3ZnO-P, 2) HDPE-MA-3CNCs-3ZnO-F, 3) HDPE-MA-5CNCs-5ZnO-P, and 4) HDPE-MA-5CNCs-5ZnO-F.

ranges, entangled chains can relax over more time, resulting in a lower modulus. At higher frequencies, entangled chains do not have enough time to relax back, and this would result in an increase in the moduli [45]. Furthermore, general values for loss modulus were higher than storage modulus for all formulations, signifying an overall viscous behavior of the polymer nanocomposites. As a consequence of the large differences found in these values for virgin HDPE and MAPE at 180 C, there can be differences in the overall storage and loss moduli of the composites HDPE and MAPE [46–49]. dummy citation Fig. 6

3.4. Dynamic mechanical analysis (DMA)

DMA studies the viscoelastic properties of the nanocomposites subjected to a periodic loading in various temperature ranges. Interactions between the nanofillers and the polymer chains can result in a different viscoelastic behavior compared to the virgin polymer. The storage modulus is associated with the polymer elastic properties (Young's modulus), while the loss modulus is associated with their viscous properties and their energy dissipation due to chain mobility. Tan δ is the ratio of loss modulus to storage modulus and represents the contribution of either of those behaviors in viscoelastic materials [50]. For comparison, storage modulus for all samples at two different temperatures, loss modulus at 50 °C, and tan δ peak intensity are shown in Table 2 and **Fig. 7**.

Storage modulus of HDPE-MA formulations were higher than that of virgin HDPE. This trend was consistent even at high temperatures. This can be attributed to the enhanced interactions and modified stress and load transfers between fibers and matrix and reinforcing effect of the CNCs [51,52]. As the percentage of nanofillers increased, the moduli started to decrease as a result of weaker interactions and agglomerations of the CNCs-ZnO in HDPE (in agreement with SEM images) [53]. Increased nanofiller concentration decreased the tan δ values marginally probably because of an increase in interactions (explain which kind of interaction, is it molecular chain locking or bonding) between the polymer chains and CNCs-ZnO, which restricted the amorphous chains' mobility. [54].

The incorporation of nanofillers in MAPE slightly decreased the values of storage modulus compared to the neat MAPE, particularly for the formulations where CNCs-ZnO was used as a film. This indicates that the nanocomposites have a decreased stiffness. A slight reduction in Tan δ peak intensity was observed, which may indicate the immobilization of polymer chains in the presence of nanofillers, and the reduced energy dissipation function.

3.5. Mechanical testing

The mechanical properties of the samples were evaluated through tensile test for virgin HDPE, MAPE and their nanocomposites. Results are summarized in Table 3. Stress-strain curves are shown in **Fig. 8**. Maximum tensile stress values were similar among pure HDPE and HDPE-MA nanocomposites. Tensile stress in MAPE nanocomposites was higher for some formulation compared to the virgin MAPE. Specifically, MAPE composites with 3 wt.% and 5 wt.% film fillers had an increased tensile strength compared to virgin MAPE (up to 46%, $p < 0.05$) and in

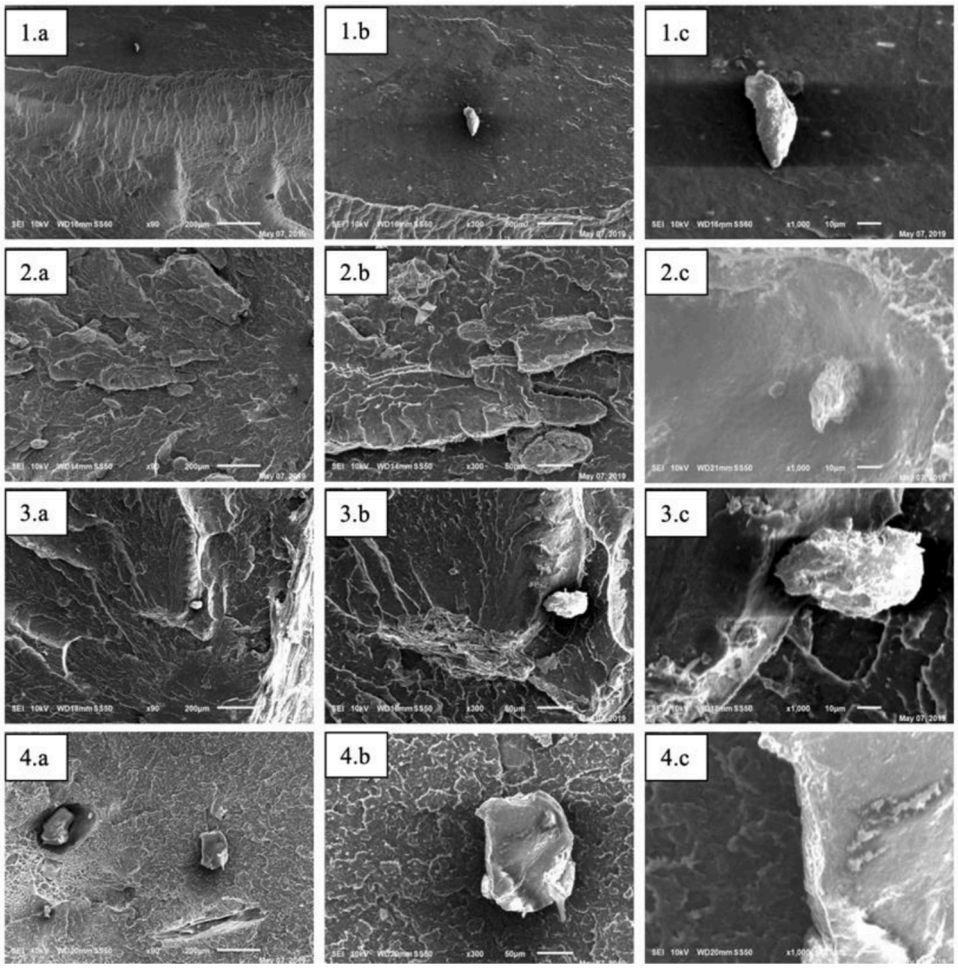

Fig. 4. SEM micrographs at three magnifications: a) 90X, b) 300X, c) 1000X for MAPE nanocomposites 1) MAPE-3CNCs-3ZnO-P, 2) MAPE-3CNCs-3ZnO-F, 3) MAPE-5CNCs-5ZnO-P, and 4) MAPE-5CNCs-5ZnO-F.

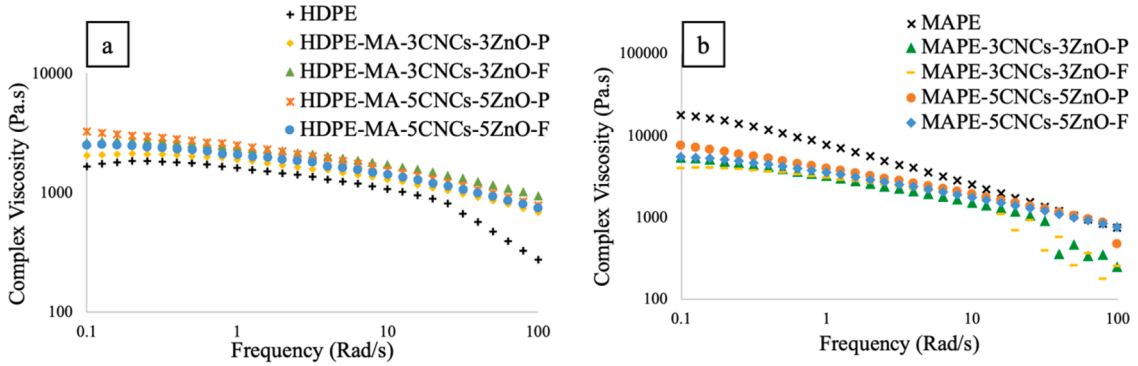

Fig. 5. Complex viscosity from rheology: a) Complex viscosity for HDPE-MA and nanocomposites, b) Complex viscosity for MAPE and nanocomposites. Y axis values are presented at logarithmic scale.

fact the highest tensile values of all the formulations. However, MAPE composites with 3 wt.% and 5 wt.% powder nanofillers had similar tensile strength to virgin MAPE. HDPE had a higher tensile stress than MAPE. In MAPE formulations, poorly dispersed film nanofillers can act as impurities in the polymer matrix and lead to increases in maximum tensile strength in composites. According to several studies, agglomerations of nanosized impurities in neat polymers can lead to an increase in the strength of the polymer by causing bonding between the polymer chains [55–57]. However, it worth noting that zinc oxide particles are shown to have a negative impact on polymers chains and cause a reduction to the molecular weight of the resulting composite [23]. This effect has the potential to cause a reduction in the overall strength of composites. The consistent tensile strength values in HDPE-MA composites may be due to the more uniform dispersion of the nanofiller where CNCs and ZnO have opposing effects on polymer matrix and composites end up with similar strength values to the virgin polymer. Other studies have also shown no to little changes in the tensile properties of HDPE with the addition of CNCs (above 1.5 wt.%) in the presence of polyethylene oxide compatibilizer [58,59]. Some studies with composites of surface-treated CNCs and low-density polyethylene,

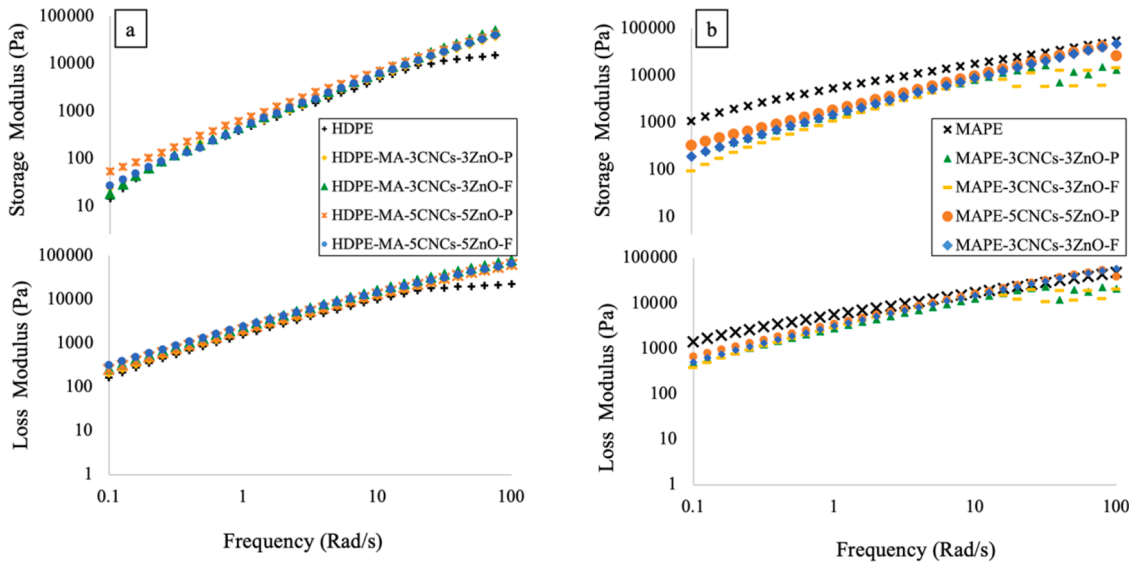

Fig. 6. Dynamic mechanical properties from rheology: a) Storage and loss moduli for HDPE-MA and its nanocomposites in a frequency sweep, b) Storage and loss moduli for MAPE and its nanocomposites in a frequency sweep. Y axis values are presented at logarithmic scale. After here, the figures have their correct caption but I am inserting them to make sure.

Table 2
Dynamic mechanical properties of HDPE and nanocomposites obtained from DMA.

Formulations	Storage modulus (MPa) 50 (°C)	100 (°C)	Loss modulus (MPa) 50 (°C)	Tan δ peak intensity
Virgin HDPE	759	178	118	0.32
MAPE	778	220	122	0.32
HDPE-MA-3CNCs-3ZnO-P	791	228	130	0.28
HDPE-MA-5CNCs-5ZnO-P	771	223	140	0.29
HDPE-MA-3CNCs-3ZnO-F	866	248	126	0.30
HDPE-MA-5CNCs-5ZnO-F	860	210	140	0.32
MAPE-3CNCs-3ZnO-P	766	228	100	0.29
MAPE-5CNCs-5ZnO-P	794	247	115	0.31
MAPE-3CNCs-3ZnO-F	650	184	113	0.31
MAPE-5CNCs-5ZnO-F	717	211	125	0.32

have reported increased tensile strength with additions of nanofillers most likely due to enhanced crystallinity, interfacial adhesion, and chain mobility of the matrix [59–61].

Young's modulus values were similar among HDPE and its nanocomposites. MAPE composites with 3 wt.% and 5 wt.% film fillers had similar Young's moduli to virgin MAPE, but MAPE composites with 3 wt.% and 5 wt.% powder nanofillers had lower Young's moduli compared to virgin MAPE (up to -20%, $p < 0.05$). This observation could be due to poor dispersion between nanofillers and the MAPE matrix in these formulations, which can cause polymer chain scission reaction and weak interfacial bonding between nanofillers and the MAPE matrix [12,62]. Especially, aggregated zinc oxide particles can cause chain scission reaction and reduce the molecular weight of the composites [23]. Overall, Young's modulus values were similar among HDPE-MA and MAPE composites.

Elongation at the maximum tensile stress was higher in HDPE-MA composites compared to virgin HDPE (up to 20%, $p < 0.05$), except for the 5 wt.% film formulation, which had a similar value to HDPE. Elongation at break was similar among the HDPE-MA nanocomposites and the virgin polymer, although a not-statistically-significant trend of lower elongation at break was observed in formulations with 5 wt.% nanofillers. Addition of nanofillers in MAPE very slightly increased MAPE's elongation up to 7% at maximum tensile strength, although it was not statistically significant. Elongation at break was similar among the MAPE nanocomposites and virgin MAPE. Overall, elongation at break was higher for HDPE formulations.

It is important to note that the DMA results generally concurs with the tensile test results. This is because the samples with a higher

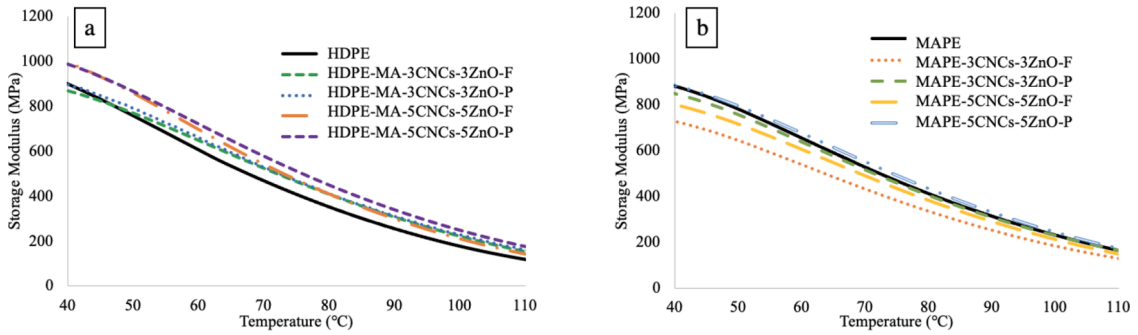

Fig. 7. Dynamic mechanical properties from DMA: a) Storage modulus for HDPE-MA and its nanocomposites in different temperatures, b) Storage modulus for MAPE and its nanocomposites in different temperatures.

Table 3
Tensile properties of composite samples and polymers in direct feeding method.

Formulations	Maximum tensile stress (MPa)	Young's modulus (Mpa)	Elongation at max tensile stress (%)
Virgin HDPE	22.1 ± 4.3^{b}	555 ± 55^{a}	11.6 ± 2.2^{b}
MAPE	18.3 ± 0.4^{cd}	579 ± 8^{a}	13.6 ± 0.5^{ab}
HDPE-MA-3CNCs-3ZnO-P	20.6 ± 2.6^{bc}	568 ± 7^{a}	13.2 ± 1.0^{ab}
HDPE-MA-5CNCs-5ZnO-P	20.0 ± 2.8^{bcd}	572 ± 58^{c}	13.1 ± 0.3^{ab}
HDPE-MA-3CNCs-3ZnO-F	19.2 ± 1.7^{bcd}	575 ± 36^{a}	8.9 ± 2.9^{c}
HDPE-MA-5CNCs-5ZnO-F	$20.7 \pm 2.8^{b\ c}$	571 ± 67^{a}	13.9 ± 1.9^{a}
MAPE-3CNCs-3ZnO-P	17.4 ± 1.5^{d}	467 ± 72^{bc}	13.2 ± 1.2^{ab}
MAPE-5CNCs-5ZnO-P	17.5 ± 1.0^{d}	401 ± 60^{c}	15.0 ± 1.4^{a}
MAPE-3CNCs-3ZnO-F	25.2 ± 0.5^{a}	503 ± 55^{ab}	15.0 ± 0.2^{a}
MAPE-5CNCs-5ZnO-F	26.8 ± 0.9^{a}	559 ± 21^{a}	15.0 ± 0.4^{a}

*Same superscript letters within the same column are not significantly different. Data are represented as mean and standard deviation.

modulus of storage exhibited a higher Young's modulus, indicative of stronger fiber and matrix interactions. Additionally, the addition of nanofillers to the MAPE matrix resulted in a decrease in the stiffness of the composite samples as well as a decrease in Young's modulus. In general, samples that have lower stiffness have higher toughness energy and a greater proportion of strain. [63,64].

The data in **Fig. 8a** shows that addition of nanofillers in HDPE did not the change mechanical properties of the polymer but increased the elongation at maximum tensile strength, whereas in Fig. 8b addition of nanofillers in MAPE based composites increased tensile strength for formulations with 3 wt.% and 5 wt.% film fillers, decreased young's modulus for formulations with 3 wt.% and 5 wt.% powder fillers and did not change elongation at maximum tensile strength.

4. Conclusion

In this work, we sought to investigate physico-mechanical properties of HDPE nanocomposites with CNCs and ZnO as nanofillers, prepared via direct feeding of coupling agent MA. Specifically, we explored the impact of adding MA (both directly or grafted on HDPE backbone) on the dispersion quality of CNCs and ZnO nanofillers (in film and powder forms) in HDPE.

- The FTIR spectra demonstrated successful coupling effect of MA between HDPE and CNCs, especially in HDPE-MA composites and successful grafting of ZnO on CNCs.
- According to SEM images at 1000X magnification, HDPE-MA nanocomposites containing 3 and 5 wt.% powder nanofillers showed little to no agglomeration of nanofillers, whereas formulations with film nanofillers and all MAPE nanocomposites showed a predominant presence of CNCs-ZnO aggregates.
- Rheology showed higher complex viscosity in the presence of nanofillers in HDPE-MA, indicating a higher melt strength of these formulations. Complex viscosity dropped in MAPE nanocomposites compared to the MAPE polymer, most likely due to presence of peroxide.
- As demonstrated by both DMA and rheology, addition of nanofillers in HDPE-MA composites increased loss and storage moduli compared to virgin HDPE, indicating an enhanced stress transfer and adhesion between the fiber and matrix in these formulations. Loss and storage moduli declined in MAPE nanocomposites compared to the MAPE polymer.
- Addition of nanofillers in HDPE did not the change mechanical properties of the polymer but increased the elongation at maximum tensile strength by up to 20%. Addition of nanofillers in MAPE increased tensile strength for formulations with 3 wt.% and 5 wt.% film fillers up to 46%, decreased Young's modulus for formulations with 3 wt.% and 5 wt.% powder fillers up to -20% and did not change elongation at maximum tensile strength.

CRediT authorship contribution statement

Ghazal Vahidi: Methodology, Data curation, Manufacturing composites, Formal analysis, Original draft preparation. **Dilpreet Bajwa:** Conceptualization, Supervision, Writing reviewing and editing, Funding acquisition. **Jamileh Shojaeiarani:** Methodology, Writing reviewing and editing. **Nicole Stark:** Conceptualization, Material resources, Validation, Reviewing

All authors contributed to the discussion, reviews, and approval of the manuscript for publication.

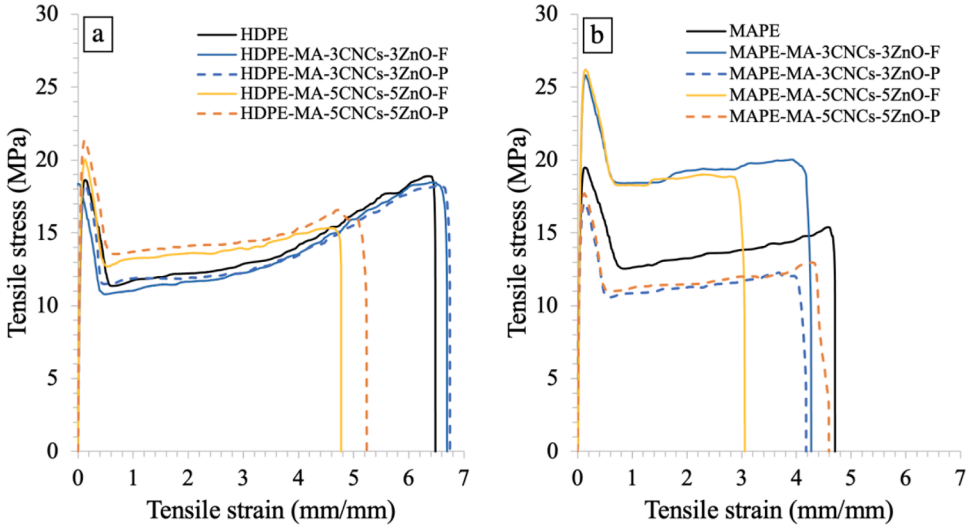

Fig. 8. Tensile properties of composite samples and polymers in direct feeding method from representative data, a) HDPE composites with direct feeding, b) MAPE composites.

Declaration of Competing Interest

The authors declare that they have no known competing financial interests or personal relationships that could have appeared to influence the work reported in this paper.

Acknowledgments

This research work is funded by USDA-NIFA, grant number 20176702233155.

References

[1] A. Kalam, R. Kamarudzaman, K.M. Hyie, A. Jumahat, N.L.A. Rahman, The role of secondary filler on fracture toughness and impact strength of HDPE/Clay nanocomposites, Pertanika J. Sci. Technol. 25 (2017) 95–104.
[2] D.L. Francisco, L.B. Paiva, W. Aldeia, Advances in polyamide nanocomposites: a review, Polym. Compos. 40 (3) (2019) 851–870.
[3] S. Coiai, E. Passaglia, A. Pucci, G. Ruggeri, Nanocomposites based on thermoplastic polymers and functional nanofiller for sensor applications, Materials (Basel) 8 (6) (2015) 3377–3427.
[4] J. Shojaeiarani, D.S. Bajwa, N.M. Stark, S.G. Bajwa, Rheological properties of cellulose nanocrystals engineered polylactic acid nanocomposites, Compos. Part B Eng. 161 (2019) 483–489.
[5] N.S. Yatigala, D.S. Bajwa, S.G. Bajwa, Compatibilization improves physico-mechanical properties of biodegradable biobased polymer composites, Compos. Part A 107 (2018) 315–325.
[6] S. Rimal, R. Rowe, R. Bathurst, Durability of fluorinated high density polyethylene (f-HDPE) geomembrane exposed to hydrocarbons in the arctic, 60th Canadian G (2007).
[7] T. Paunikallio, M. Suvanto, T. Pakkanen, Grafting of 3-(trimethoxysilyl) propyl methacrylate onto polypropylene and use as a coupling agent in viscose fiber/polypropylene composites, React. Funct. Polym. 68 (3) (2008) 797–808.
[8] M. Abdelmouleh, S. Boufi, M.N. Belgacem, A. Dufresne, Short natural-fibre reinforced polyethylene and natural rubber composites: effect of silane coupling agents and fibres loading, Compos. Sci. Technol. 67 (7–8) (2007) 1627–1639.
[9] M. Bengtsson, K. Oksman, Silane crosslinked wood plastic composites: processing and properties, Compos. Sci. Technol. 66 (13) (2006) 2177–2186.
[10] L. Heux, G. Chauve, C. Bonini, Nonflocculating and chiral-nematic self-ordering of cellulose microcrystals suspensions in nonpolar solvents, Langmuir 16 (21) (2000) 8210–8212.
[11] J.R. Capadona, et al., A versatile approach for the processing of polymer nanocomposites with self-assembled nanofibre templates, Nat. Nanotechnol. 2 (12) (2007) 765.
[12] D. Jun, Z. Guomin, P. Mingzhu, Z. Leilei, L. Dagang, Z. Rui, Crystallization and mechanical properties of reinforced PHBV composites using melt compounding: effect of CNCs and CNFs, Carbohydr. Polym. 168 (2017) 255–262.
[13] H. Gao, Y. Xie, R. Ou, Q. Wang, Grafting effects of polypropylene/polyethylene blends with maleic anhydride on the properties of the resulting wood–plastic composites, Compos. Part A 43 (1) (2012) 150–157.
[14] F. Wang, L. Dai, T. Ge, C. Yue, Y. Song, α-methylstyrene-assisted maleic anhydride grafted poly (lactic acid) as an effective compatibilizer affecting properties of microcrystalline cellulose/poly (lactic acid) composites, Express Polym. Lett. 14 (6) (2020).
[15] M. Pöllänen, M. Suvanto, T.T. Pakkanen, Cellulose reinforced high density polyethylene composites—Morphology, mechanical and thermal expansion properties, Compos. Sci. Technol. 76 (2013) 21–28.
[16] P. Kosaka, Y. Kawano, H. Petri, M. Fantini, D. Petri, Structure and properties of composites of polyethylene or maleated polyethylene and cellulose or cellulose esters, J. Appl. Polym. Sci. 103 (1) (2007) 402–411.
[17] D.S. Bajwa, J. Shojaeiarani, J.D. Liaw, S.G. Bajwa, Role of hybrid nano-zinc oxide and cellulose nanocrystals on the mechanical, thermal, and flammability properties of poly (Lactic Acid) polymer, J. Compos. Sci. 5 (2) (2021) 43.
[18] X. Liang, et al., Design and synthesis of porous M-ZnO/CeO2 microspheres as efficient plasmonic photocatalysts for nonpolar gaseous molecules oxidation: insight into the role of oxygen vacancy defects and M= Ag, Au nanoparticles, Appl. Catal. B 260 (2020), 118151.
[19] A. Prasert, S. Sontikaew, D. Sriprapai, S. Chuangchote, Polypropylene/ZnO nanocomposites: mechanical properties, photocatalytic dye degradation, and antibacterial property, Materials (Basel) 13 (4) (2020) 914.
[20] S. Hokkanen, A. Bhatnagar, M. Sillanpää, A review on modification methods to cellulose-based adsorbents to improve adsorption capacity, Water Res. 91 (2016) 156–173.
[21] P. Lu, Y.L. Hsieh, Preparation and properties of cellulose nanocrystals: rods, spheres, and network, Carbohydr. Polym. 82 (2) (2010) 329–336.
[22] I. Grigoriadou, E. Pavlidou, K.M. Paraskevopoulos, Z. Terzopoulou, D.N. Bikiaris, Comparative study of the photochemical stability of HDPE/Ag composites, Polym. Degrad. Stab. 153 (2018) 23–36.
[23] J. Shojaeiarani, D. Bajwa, L. Jiang, J. Liaw, K. Hartman, Insight on the influence of nano zinc oxide on the thermal, dynamic mechanical, and flow characteristics of Poly (lactic acid)–zinc oxide composites, Polym. Eng. Sci. (2019).
[24] A. International, Standard Test Method For Tensile Properties of Plastics, ASTM international, 2014.
[25] A. International, Standard Test Method For plastics: Dynamic Mechanical properties: in Tension, ASTM International, 2001.
[26] D. Samsudin, H. Ismail, N. Othman, Z.A.A. Hamid, Comparative study of glut palmitate salt and polyethylene grafted maleic anhydride compatibilizer on the properties of silica filled high-density polyethylene composites, Polym. Test. 52 (2016) 104–110.
[27] M. Mehrabzadeh, M.R. Kamal, and G. Quintanar, "Maleic anhydride grafting onto HDPE by *in situ* reactive extrusion and its effect on intercalation and mechanical properties of HDPE/clay nanocomposites," 2009.
[28] E. Manaila, M.D. Stelescu, G. Craciun, L. Surdu, Effects of benzoyl peroxide on some properties of composites based on hemp and natural rubber, Polym. Bull. 71 (8) (2014) 2001–2022.
[29] X.X. Guo, et al., Rapid determination and chemical change tracking of benzoyl peroxide in wheat flour by multi-step IR macro-fingerprinting, Spectrochim. Acta Part A 154 (2016) 123–129.
[30] A. Oromiehie, H. Ebadi-Dehaghani, S. Mirbagheri, Chemical modification of polypropylene by maleic anhydride: melt grafting, characterization and mechanism, Int. J. Chem. Eng. Appl. 5 (2) (2014) 117.
[31] M. Kazayawoko, J. Balatinecz, R. Woodhams, Diffuse reflectance Fourier transform infrared spectra of wood fibers treated with maleated polypropylenes, J. Appl. Polym. Sci. 66 (6) (1997) 1163–1173.
[32] A. Sato, D. Kabusaki, H. Okumura, T. Nakatani, F. Nakatsubo, H. Yano, Surface modification of cellulose nanofibers with alkenyl succinic anhydride for high-density polyethylene reinforcement, Compos. Part A 83 (2016) 72–79.
[33] X. Kai, T. Yang, S. Shen, R. Li, TG-FTIR-MS study of synergistic effects during co-pyrolysis of corn stalk and high-density polyethylene (HDPE), Energy Convers. Manag. 181 (2019) 202–213.
[34] K. Zhang, et al., Improve the flame retardancy of cellulose fibers by grafting zinc ion, Carbohydr. Polym. 136 (2016) 121–127.
[35] J. Shojaeiarani, D.S. Bajwa, N.M. Stark, Green esterification: a new approach to improve thermal and mechanical properties of poly (lactic acid) composites reinforced by cellulose nanocrystals, J. Appl. Polym. Sci. (2018) 46468.
[36] G.F. de Lima, A.G. de Souza, D.S. Rosa, Effect of adsorption of polyethylene glycol (PEG), in aqueous media, to improve cellulose nanostructures stability, J. Mol. Liq. 268 (2018) 415–424.
[37] S. Sundararajan, A.B. Samui, P.S. Kulkarni, Shape-stabilized poly (ethylene glycol) (PEG)-cellulose acetate blend preparation with superior PEG loading via microwave-assisted blending, Sol. Energy 144 (2017) 32–39.
[38] Y. Li, R. Liu, Y. Huang, Synthesis and phase transition of cellulose-graft-poly (ethylene glycol) copolymers, J. Appl. Polym. Sci. 110 (3) (2008) 1797–1803.
[39] J. Shojaeiarani, D.S. Bajwa, N.M. Stark, Spin-coating: a new approach for improving dispersion of cellulose nanocrystals and mechanical properties of poly (lactic acid) composites, Carbohydr. Polym. 190 (2018) 139–147.
[40] R. Rezanavaz, M. Razavi Aghjeh, A. Babaluo, Rheology, morphology, and thermal behavior of HDPE/clay nanocomposites, Polym. Compos. 31 (6) (2010) 1028–1036.
[41] S.K. Swain, A.I. Isayev, Effect of ultrasound on HDPE/clay nanocomposites: rheology, structure and properties, Polymer (Guildf) 48 (1) (2007) 281–289.
[42] S. Mir, T. Yasin, H.M. Siddiqi, G. Murtaza, Thermal, rheological, mechanical and morphological behavior of high density polyethylene and carboxymethyl cellulose blend, J. Polym. Environ. 25 (4) (2017) 1011–1020.
[43] Y.C. Ching, et al., Rheological properties of cellulose nanocrystal-embedded polymer composites: a review, Cellulose 23 (2) (2016) 1011–1030.
[44] S.K. Muniyandi, J. Sohaili, A. Hassan, Accelerated weathering properties of compatibilized composites made from recycled HDPE and nonmetallic printed circuit board waste, J. Appl. Polym. Sci. 133 (11) (2016).
[45] S. Mir, T. Yasin, P.J. Halley, H.M. Siddiqi, T. Nicholson, Thermal, rheological, mechanical and morphological behavior of HDPE/chitosan blend, Carbohydr. Polym. 83 (2) (2011) 414–421.
[46] J.S. Sefadi, Preparation and properties of conductive polymer nanocomposites, University of the Free State (Qwaqwa Campus), 2015.
[47] X. Hao, et al., Interfacial adhesion mechanisms of ultra-highly filled wood fiber/polyethylene composites using maleic anhydride grafted polyethylene as a compatibilizer, Mater. Des. 212 (2021), 110182.
[48] A.A. Al-Juhani, Rheology, mechanical properties, and thermal stability of maleated polyethylene filled with nanoclays, J. Nanomater. 2015 (2015).
[49] L. Xie, et al., Preparation and properties of long chain branched high-density polyethylene based on nano-SiO 2 grafted glycidyl methacrylate, RSC Adv. 9 (2) (2019) 1123–1133.
[50] F. Ferreira, et al., Influence of carbon nanotube concentration and sonication temperature on mechanical properties of HDPE/CNT nanocomposites, Fuller. Nanotubes Carbon Nanostruct. 25 (9) (2017) 531–539.
[51] X. Xu, F. Liu, L. Jiang, J. Zhu, D. Haagenson, D.P. Wiesenborn, Cellulose nanocrystals vs. cellulose nanofibrils: a comparative study on their microstructures and effects as polymer reinforcing agents, ACS Appl. Mater. Interfaces 5 (8) (2013) 2999–3009.
[52] D. Oliveira de Castro, E. Frollini, A. Ruvolo-Filho, A. Dufresne, Green polyethylene" and curauá cellulose nanocrystal based nanocomposites: effect of vegetable oils as coupling agent and processing technique, J. Polym. Sci. Part B Polym. Phys. 53 (14) (2015) 1010–1019.
[53] K.Z.C. da Cruz, A.C. Casagrande, O.L. Casagrande Jr, High-density polyethylene/expanded graphite nanocomposites produced by polymerization-filling technique using an industrial heterogeneous catalyst, J. Polym. Sci. Part A Polym. Chem. 55 (7) (2017) 1260–1267.

[54] L.P. Novo, A.A. da Silva Curvelo, A.J.F. Carvalho, Nanocomposites of acid free CNC and HDPE: dispersion from solvent driven by fast crystallization/gelation, J. Mol. Liq. 266 (2018) 233–241.
[55] M.S. Mozumder, A.H.I. Mourad, A. Mairpady, H. Pervez, M.E. Haque, Effect of TiO_2 Nanofiller Concentration on the Mechanical, Thermal and Biological Properties of HDPE/TiO_2 Nanocomposites, J. Mater. Eng. Perform. 27 (5) (2018) 2166–2181.
[56] J. Iskoe, F. Lange, E. Diaz, Effect of selected impurities on the high temperature mechanical properties of hot-pressed silicon nitride, J. Mater. Sci. 11 (5) (1976) 908–912.
[57] Y. Wang, S. Cheng, Q. Wei, E. Ma, T. Nieh, A. Hamza, Effects of annealing and impurities on tensile properties of electrodeposited nanocrystalline Ni, Scr. Mater. 51 (11) (2004) 1023–1028.
[58] N. Inai, A. Lewandowska, O. Ghita, S. Eichhorn, Interfaces in polyethylene oxide modified cellulose nanocrystal-polyethylene matrix composites, Compos. Sci. Technol. 154 (2018) 128–135.
[59] M. Pereda, N.E. Kissi, A. Dufresne, Extrusion of polysaccharide nanocrystal reinforced polymer nanocomposites through compatibilization with poly (ethylene oxide), ACS Appl. Mater. Interfaces 6 (12) (2014) 9365–9375.
[60] N. Volk, R. He, K. Magniez, Enhanced homogeneity and interfacial compatibility in melt-extruded cellulose nano-fibers reinforced polyethylene via surface adsorption of poly (ethylene glycol)-block-poly (ethylene) amphiphiles, Eur. Polym. J. 72 (2015) 270–281.
[61] M. Nagalakshmaiah, F. Pignon, N. El Kissi, A. Dufresne, Surface adsorption of triblock copolymer (PEO–PPO–PEO) on cellulose nanocrystals and their melt extrusion with polyethylene, RSC Adv. 6 (70) (2016) 66224–66232.
[62] J. Shojaeiarani, M. Hosseini-Farid, D. Bajwa, Modeling and experimental verification of nonlinear behavior of cellulose nanocrystals reinforced poly (lactic acid) composites, Mech. Mater. (2019).
[63] J.M. da Silva, S.V. Coutinho, R.K. Diniz, A.N. Almeida, M.E. Lima, F.de C. Fim, Evaluation of the Mechanical and Thermal Properties of Blended (HDPE/UHMWPE) Nanocomposites with Graphite Nanosheets (GNS), Macromol. Symp. 383 (1) (2019).
[64] B. De Menezes, et al., Effects of octadecylamine functionalization of carbon nanotubes on dispersion, polarity, and mechanical properties of CNT/HDPE nanocomposites, J. Mater. Sci. 53 (20) (2018) 14311–14327.